photochem

MDPI

Article

Modeling the Unimolecular Decay Dynamics of the Fluorinated Criegee Intermediate, CF_3CHOO

Lily M. Guidry,[1,#,†] Courtney A. Poirier,[1,2,†] Jordyn M. Ratliff,[1,#] Ernest Antwi,[3] Barbara Marchetti,[1] and Tolga N. V. Karsili[1,*]

[1]Department of Chemistry, University of Louisiana at Lafayette, Lafayette, LA 70504, USA
[2]Regional Application Center, NASA/University of Louisiana at Lafayette, Lafayette, LA 70506, USA
* Correspondence: to whom correspondence should be addressed, tolga.karsili@louisiana.edu
[#]authors contributed as undergraduate research students.
†authors contributed equally.

Abstract: When volatile alkenes are emitted into the atmosphere, they are rapidly removed by oxiding agents such as hydroxyl radicals and ozone. The latter reaction is termed ozonolysis and is an important source of Criegee intermediates (CIs), *i.e.*, carbonyl oxides that are implicated in enhancing the oxidizing capacity of the troposphere. These CIs aid in the formation of lower volatility compounds that typically condense to form secondary organic aerosols. CIs have attracted vast attention in the past two decades. Despite this, the effect of substitution on the ground and excited state chemistries of CIs is still not well studied. Here we extend our knowledge learned from outcomes of prior studies on CIs by CF_3 substitution. The resulting CF_3CHOO molecule is a CI that may be formed from the ozonolysis of hydrofluoroolefines (HFOs). Our results show that the ground state unimolecular decay should be less reactive and thus more persistent in the atmosphere than the non-fluorinated analogue. The excited state dynamics, however, are predicted to occur on an ultrafast timescale. The results are discussed in the context of ways in which our studies advance synthetic chemistry, as well as processes relevant to the atmosphere.

Introduction

Hydrofluorooelfins (HFOs) are unsaturated organofluorides used in modern day refrigerants.[1–3] These fourth generation refrigerants are of particular interest, as they have been manufactured to replace harmful chlorofluorocarbons (CFCs), hydrochlorofluorocarbons (HCFCs), and hydrofluorocarbons (HFCs). HFOs are preferred over CFCs, HCFCs, and HFCs due to their very low global warming and zero ozone depletion potentials.[4,5] This is a consequence of their short lifetimes in the troposphere, as they undergo oxidation via OH and Cl radicals, as well as with O_3.[6,7]

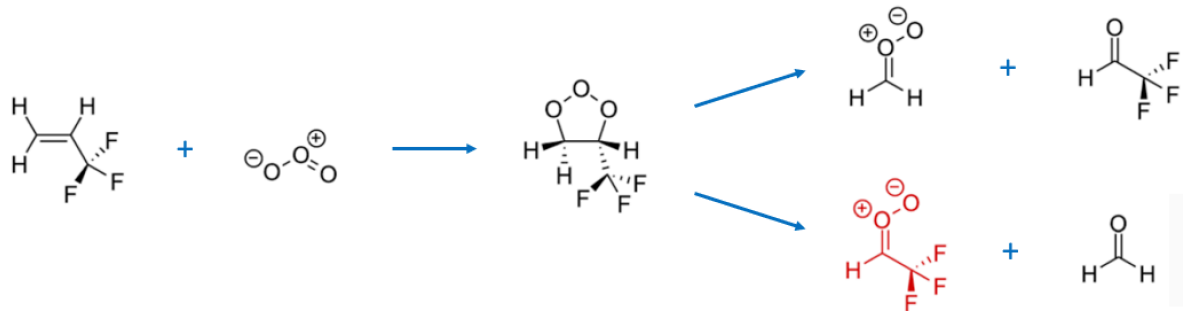

Figure 1. Schematic reaction path displaying the ozonolysis of the HFO-1243zf refrigerant. The molecule of interest in this study is shown in red (trifluoroacetaldehyde oxide – CF_3CHOO).

While much is known about HFO molecules themselves, little is known about the (photo)reactivities of their oxidation products. In the atmosphere, HFOs react with ozone through ozonolysis across an olefinic C=C bond. Fig. 1 provides an example of such a reaction with a common HFO refrigerant, tetrafluoropropene (HFO-1243zf), wherein ozonolysis occurs via a [3+2]-cycloaddition of ozone across the C=C double bond of HFO-1243zf, resulting in the formation of a primary ozonide (POZ). Since the [3+2]-cycloaddition reaction is highly exothermic, the POZ is formed highly internally excited, decaying faster than the timescale for collisionally energy relaxation that would otherwise form a stabilized POZ. Its unimolecular decay occurs via cleavage of the five-membered ring center C-C and one of the two O-O bonds, yielding the two distinct products: H_2COO + CF_3CHO or CF_3CHOO + H_2CO. These H_2COO and CF_3CHOO products are known as Criegee intermediates (CIs), which are recognized for enhancing the oxidating capacity of the atmosphere and are implicated in secondary organic aerosol formation.[8–11]

Non-fluorine containing CIs (such as H_2COO) are formed in the atmosphere when volatile alkenes undergo ozonolysis. The simplest alkyl-substituted CI is acetaldehyde oxide (CH_3CHOO), formed from the ozonolysis of molecules such as propene. It may be formed in two *syn-* and *anti-* conformers. CH_3CHOO can undergo unimolecular decay via intramolecular hydrogen-atom transfer, forming vinyl hydroperoxide (VHP), which subsequently decays to form vinoxy and OH radicals.[10,12–14] While this process is favored in *syn*-CH_3CHOO, *anti*-CH_3CHOO unimolecular decay is dominated by the formation of methyl dioxirane or acetic acid ($CH_3C(O)OH$) via isomerization, which decays to form CH_3CO + OH, CH_4 + CO_2, and CH_3OH + CO. CH_3CHOO, especially in the *anti-* conformation, can also undergo bimolecular chemistry with species in the troposphere, such as H_2O, SO_2, O_3, and HCOOH.[15] The photochemical properties of CH_3CHOO are also worthy of discussion.[16,17] Using UV action spectroscopy and velocity map imaging on jet-cooled CH_3CHOO, Lester and co-workers have shown through their studies that photodissociation of this molecule causes the formation of CH_3CHO + O products after excitation at $\lambda <$ 350 nm. This dissociation results in two spin-allowed channels, which are indicated by CH_3CHO (S_0) + O (^1D) and CH_3CHO (T_1) + O (^3P) products, with the latter being open for only $\lambda \leq 324$ nm. Through the use of trajectory surface hopping (TSH) molecular dynamics with energies, gradients, and non-adiabatic couplings computed "on-the-fly" using MS-CASPT2, we previously assessed the dynamics of CH_3CHOO following excitation to the S_2 state. O-O bond dissociation caused by this excitation to the S_2 state results in a branching ratio that favors the CH_3CHO (S_0) + O (^1D) asymptote.[16]

In this manuscript, we explore the effects of fluorination on ground state unimolecular decay and photodissociation dynamics of the ground state and excited state unimolecular decay of *syn-* and *anti-* CF_3CHOO.

Methodology

The ground state minimum energy geometries of CH_3CHOO and CF_3CHOO, along with their respective dioxirane products and transition states, were optimized at the m06-2x/aug-cc-pVTZ level of theory using the Gaussian computational package.[18] Using CCSD(T)-F12/cc-pVTZ-F12 level of theory, single point energy calculations were computed on the optimize structures, allowing us to obtain more accurate energies. These latter calculations were carried out in Molpro.[19,20] This combination of m06-2x/aug-cc-pVTZ//CCSD(T)-F12 has been successfully applied to develop a structure-activity relationship of the unimolecular decay kinetics of substituted Criegee intermediates.[21,22]

The fate of the excited states of CF_3CHOO were modeled using TSH and static electronic structure calculations. TSH simulations were carried out using the Newton-X computational package.[23,24] Initial conditions were acquired by using a Wigner distribution based on the B2PLYP-D3/cc-pVTZ equilibrium geometry of *syn* and *anti* CF_3CHOO and their respective harmonic normal mode wavenumbers. As shown in prior findings, this level of theory performs well in obtaining the geometries and normal modes of CIs and their associated reaction profiles.[25–32] In TSH, the nuclei were propagated by integrating

Newton's equation using the velocity Verlet method, while the electronic coordinates are treated quantum mechanically by numerically solving the time-dependent Schrodinger equation using Butcher's fifth-order Runge-Kutta method in steps of 0.025 fs.[33] Trajectories were initiated on the bright S_2 state. Energies, forces and non-adiabatic coupling matrix elements were computed on-the-fly, using the single-state, single-reference multistate complete active space second order perturbation theory (SS-SR-CASPT2) method along with the cc-pVDZ basis set. These energies/forces are computed via the BAGEL interface to Newton-X.[34,35] SS-SR-CASPT2 not only produces energies and analytical gradients at the MS-CASPT2 quality at a reduced computational cost, but also performs well near electronic state degeneracies. The SS-SR-CASPT2 calculations were based on a state-averaged complete active space self-consistent field (CASSCF) method reference wavefunction and an active space composed of 10 electrons in 8 orbitals. Additional potential energy profiles were computed in order to assess the excited state reaction paths along the O-O stretch coordinate. These were computed using Molpro, at the CASPT2/aug-cc-pVTZ level of theory, using the same 10/8 active space as the previously mentioned TSH simulations. Due to the highly multi-reference nature of the excited-state dynamics of Criegee intermediate, these methods are required for modeling the excited states of our present systems. Our previous studies have highlighted the success of SS-SR-CASPT2 is assessing the excited state dynamics and energy profiles of Criegee intermediates.

Results and Discussion

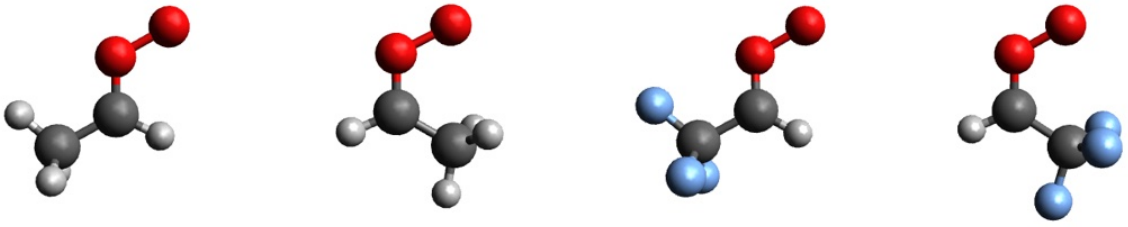

Figure 2. Minimum energy structures of *anti-* and *syn*-H_3CHOO and *anti-* and *syn*-CF_3CHOO.

Fig. 2 displays the ground state minimum energy geometry of the *syn-* and *anti-* conformers of CF_3CHOO. These conformers are distinguishable by the orientation of the terminal oxygen atom relative to the CF_3 group. *Anti*-CF_3CHOO is the most stable conformer and is predicted to be ca. 0.6 kcal mol^{-1} more stable than *syn*-CF_3CHOO – manifesting in Boltzmann populations of ca. 74 % (*anti*) and 26 % (*syn*). This observation is in contrast to CH_3CHOO,[12] which shows a preference for forming *syn-* conformers due to the weak intramolecular hydrogen-bonding interaction between the CH_3 centered H-atoms and the terminal oxygen atom. Since this interaction does not exist in *syn*-CF_3CHOO, the *anti*-CF_3CHOO shows less steric hindrance (cf. *syn*-CF_3CHOO). The equivalent energy difference between *syn-* and *anti-* CH_3CHOO is ca. 3.7 kcal mol^{-1}, with a barrier height of ca. 38 kcal mol^{-1}.

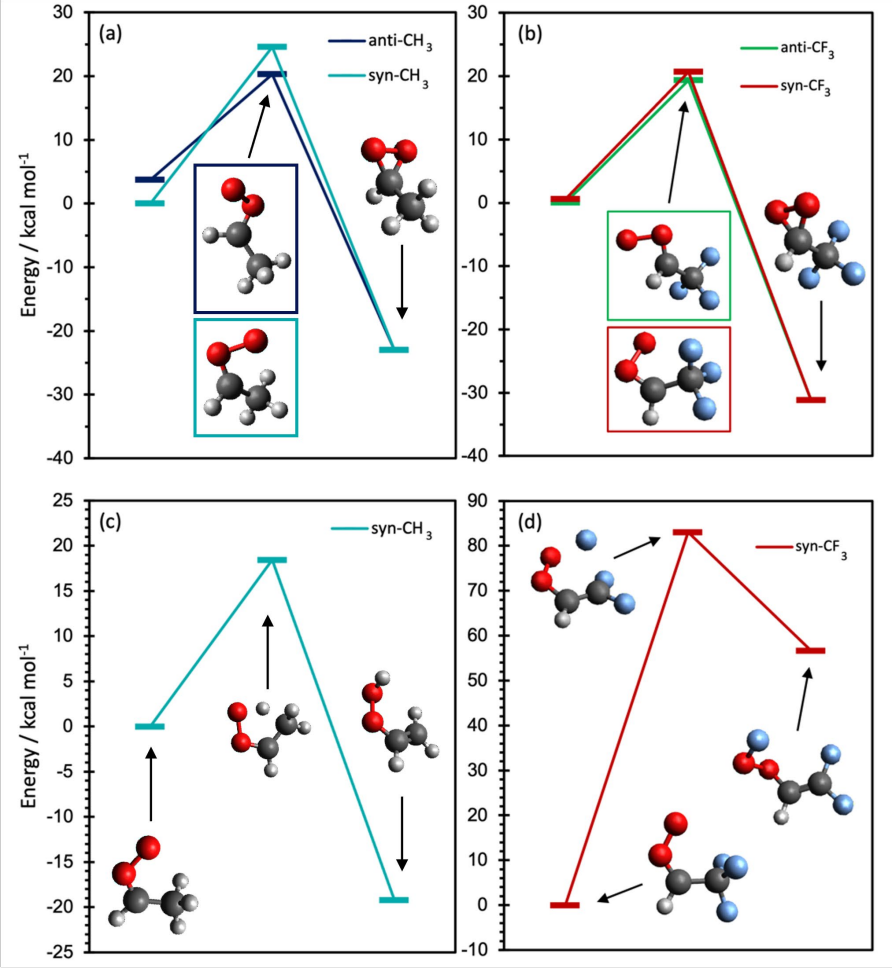

Figure 3. Reaction energy profiles associated with the unimolecular decay paths available to CH_3CHOO and CF_3CHOO; dioxirane formation in (a) CH_3CHOO and (b) CF_3CHOO, (c) 1,4-H migration in *syn*-CH_3CHOO and (d) F-migration in *syn*-CF_3CHOO. Panels (a) and (b) represent the cyclization to form dioxirane products, while (c) and (d) represent the energy profile associated with intramolecular hydrogen or fluorine atom transfer, respectively.

Guided by previous studies on the ozonolysis of CIs, CF_3CHOO is expected to undergo bimolecular chemistry with trace gases in the atmosphere or unimolecular decay either thermally or after UV-excitation. Here, we will focus on the latter two unimolecular decay paths. Figs. 3(a) and 3(c) display the energy profiles associated with the two most prominent unimolecular decay paths of CH_3CHOO – i.e., isomerization to form vinyl hydroperoxide (VHP) or dioxide, respectively. VHP formation involves 1,4-hydrogen-atom migration and is the dominant unimolecular decay path for the more stable (*syn*) conformer of CH_3CHOO, and is predicted to contains a transition state barrier of ca.18 kcal mol^{-1} – which is in excellent agreement with prior high-level quantum chemical studies.[36] The equivalent isomerization in CF_3CHOO would involve a 1,4-fluorine atom migration (Fig. 3(d)). As expected, the energy profile associated with F-atom migration contains a transition state barrier that is ca. 60 kcal mol^{-1} higher than the equivalent H-atom migration in *syn*-CH_3CHOO – manifesting from an unfavorable C-F bond fission and an equally unfavorable OF bond formation. In contrast, cyclization of CF_3CHOO to form dioxirane contains a transition state barrier that is comparable to that of CH_3CHOO (Fig. 3 (a) and (b)). We therefore expect cyclization to be the only competitive thermal removal process in CF_3CHOO, which is expected to proceed with a low rate constant. Under low humidity conditions, we expect CF_3CHOO to be long-lived when compared to the typical sub-

second atmospheric lifetime of CIs. As such, it might absorb UV radiation and become photoexcited.

Fig. 4 presents the orbitals and orbital promotions associated with electronic excitation to the S_1 and S_2 states. As with other CIs, excitation to the S_1 state arises via a $\pi^* \leftarrow n$ orbital promotion and contains zero oscillator strength. In contrast, excitation to the S_2 state involves a $\pi^* \leftarrow \pi$ electron promotion, which is the transition that dominates the near-UV absorption. This aligns with previous observations of CIs.[17]

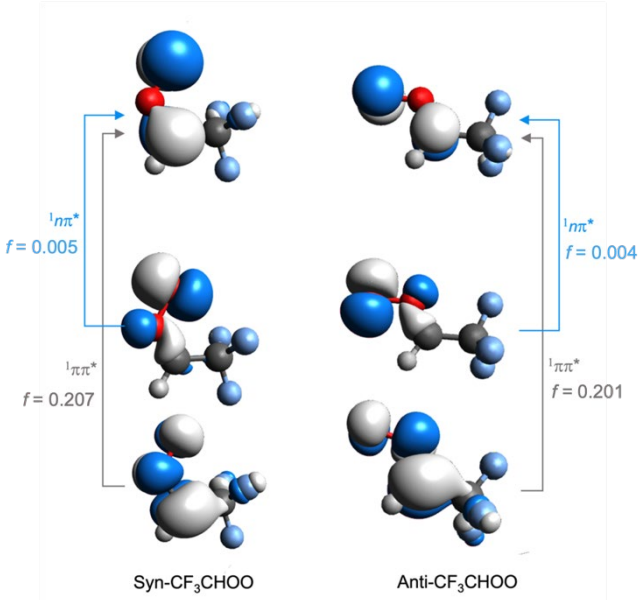

Figure 4. Orbitals and orbital promotions associated with excitation to the lowest two singlet excited electronic states of *syn-* and *anti-* CF_3CHOO.

Following excitation to the bright S_2 state, our TSH simulations (Fig. 5) reveal deactivation of the S_2 state within 40 fs. Analysis of the TSH simulations reveals that both the *syn-* and *anti-* conformers dominantly undergo O-O bond elongation within 40 fs, leading to the formation of CF_3CHO + O products with a unity quantum yield. In the higher energy *syn-* conformer (Fig. 5(b)), prompt internal conversion at early time reveals partitioning of the population to all seven electronic states. In contrast, only the S_0, S_1, S_2, S_3 and S_4 states are populated in the *anti-* conformer – *i.e.*, the lower energy conformer.

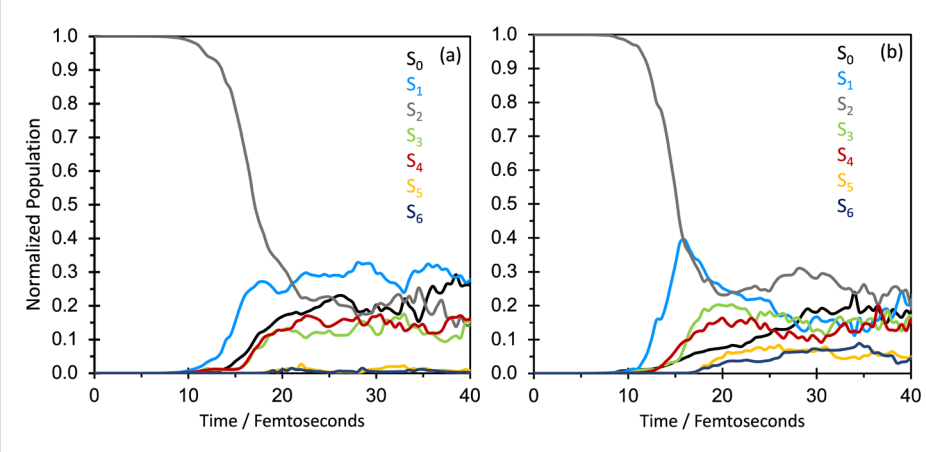

Figure 5. The time evolution of the populations for excitation to the S_2 state of (a) *anti*-CF_3CHOO and (b) *syn*-CF_3CHOO.

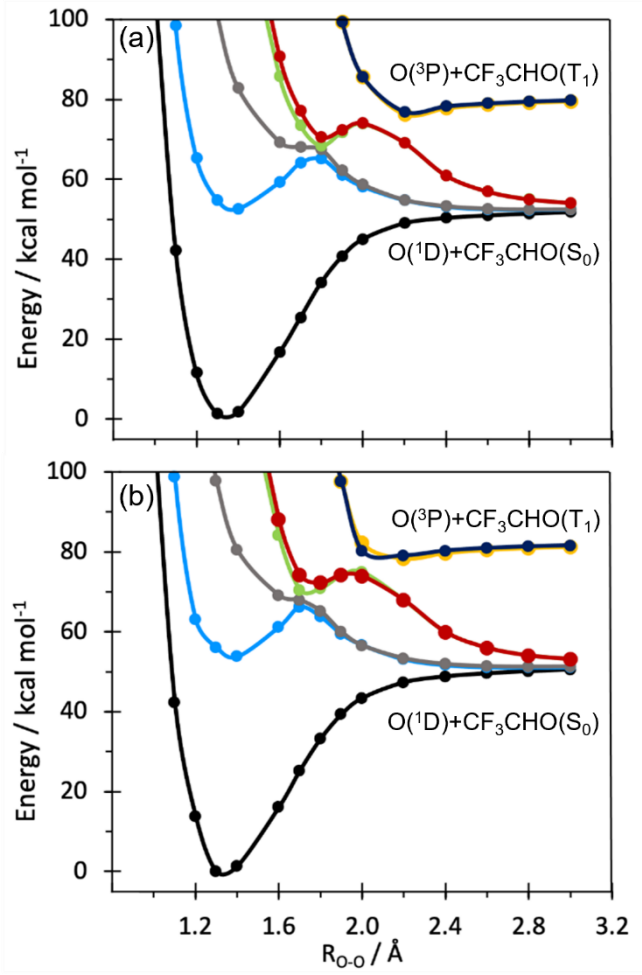

Figure 6. Adiabatic potential energy profiles along the O-O stretch coordinate for the lowest seven singlet states of (a) *anti*-CF_3CHOO and (b) *syn*-CF_3CHOO.

As the CASPT2 PE profiles along the O-O elongation coordinate (Fig. 6) reveal, the S_0, S_1, S_2, S_3 and S_4 states correlate with the lower energy asymptote, corresponding to $O(^1D) + CF_3CHO(S_0)$ products, while the S_5 and S_6 states correlate with the second asymptote, corresponding to $O(^3P) + CF_3CHO(T_1)$ products. The electronic state character of the S_0-S_6 states are the same as those reported in our earlier work,[37] which will be briefly outlined in the following text. In the former cluster of states, S_0 involves an intuitive long-range attractive interaction which arises via the interaction between the CF_3CHO centered O-2p lone pair and the vacant 2p orbital on $O(^1D)$. At long R_{OO}, this same 2p orbital is either singly or doubly occupied in the S_1-S_4 state configurations, manifesting in the long-range repulsive interaction that is observed for these states in Fig. 6. The S_5 and S_6 states contain a long-range attractive interaction, which can be understood by considering that that the T_1 state of formaldehyde is of $n\pi^*$ character, with an odd electron in the oxygen centered 2p lone pair. This odd electron forms a bonding pair with the odd electron in one of the two odd-electrons in the 2p orbital of the $O(^3P)$ atom. This agrees with previous observations of CIs photochemistry.[17] As noted in the above description, in the *anti*-conformer, a negligible portion of the starting populations partitions to the higher energy S_5 and S_6 states, manifesting in a negligible yield of $O(^3P) + CF_3CHO(T_1)$ products. In contrast, for the *syn*-conformer, ca. 15% of the initial excited population partitions across the S_5 and S_6, indicating ca. 15% yield of $O(^3P) + CF_3CHO(T_1)$ products within 40 fs. This latter observation is in line with a previous observation of the simplest CI, CH_2OO, which returns an equally low fraction of the overall population into $O(^3P) + CH_2O(T_1)$ products.[38] This observation is striking and may be plausibly explained by the weaker interaction between

S_3/S_4 and S_5/S_6 states or by a perturbation caused by the CF_3 moeity on the O atom leaving group.

The dominant nuclear motions associated with these internal conversions can be understood by assessing the PE profiles in Fig. 6, which show two important avoided crossings. The first is at R_{OO} ~ 1.7 Å which involves a four-state intersection, involving the S_1, S_2, S_3 and S_4 states. The early-time internal conversation observed in the TSH results arise via internal conversion at these crossing points. A second avoided crossing is observed at R_{OO} ~ 2.2 Å between the S_3, S_4, S_5 and S_6 states. The ultimate branching into the $O(^1D)$ + $CF_3CHO(S_0)$ and $O(^3P)$ + $CF_3CHO(T_1)$ products is governed by internal conversion at this crossing point.

Conclusions

In this article, we reported the details of the ground and excited state unimolecular decay of CF_3CHOO, which may be formed from the ozonolysis of commonly used HFOs. Unlike CH_3CHOO, the two *syn-* and *anti-* conformers of CF_3CHOO are energetically close, manifesting from the absence of hydrogen bonding that is present in *syn*-CH_3CHOO. Our results show that the unimolecular decay of CF_3CHOO is expected to follow an analogous cyclization to form dioxirane products, but with a lower energy barrier. Unlike CH_3CHOO however, *syn*-CF_3CHOO does not have an analogous hydrogen atom transfer that forms a vinyl hydroperoxide. As demonstrated in our results above, the analogous fluorine atom transfer is, as expected, unfavourable. As with other CIs, the electronic absorption of CF_3CHOO is dominated by the S_2 state, which arises via a $\pi^* \leftarrow \pi$ transition. Excitation to this state leads to prompt O-O bond fission, forming $O(^1D)$ products in both *syn*-CF_3CHOO and *anti*-CF_3CHOO. Unlike CH_2OO, the $O(^3P)$ channel is unobserved in *syn*-CF_3CHOO.

The results shed light on the expected ground and excited state chemistry of an HFO derived CI. When HFO refrigerants are emitted into the atmosphere, their primary removal is via reaction with OH radicals, but reaction with O_3 is relevant in certain environments. Our studies are also relevant to the synthetic chemistry community since the results highlight the effect of a CF_3 substitution of the ground and excited state dynamics of a substituted CI. When compared to our previous studies on CFHOO, the effect of CF_3 substitution is much less dramatic than F substitution, which is most likely due to a weaker π-perturbing effect of CF_3 *versus* F.

Our future studies will focus on the bimolecular chemistry of CF_3CHOO and how its chemistry compares to CH_3CHOO. Since some HFOs contain chlorine substituent, we would also be excited to explore the effect of chlorination on the ground and excited state chemistry of CIs.

Acknowledgments: The work reported in this article is supported by the National Science Foundation, under grant no. 2003422. C.A.P thanks the National Science Foundation (2120015) for the award of a research assistantship. Portions of this research were conducted with high performance computational resources provided by the Louisiana Optical Network Infrastructure (http://www.loni.org).

References

1 C. Mateu-Royo, J. Navarro-Esbrí, A. Mota-Babiloni, M. Amat-Albuixech and F. Molés, Thermodynamic analysis of low GWP alternatives to HFC-245fa in high-temperature heat pumps: HCFO-1224yd(Z), HCFO-1233zd(E) and HFO-1336mzz(Z), *Appl. Therm. Eng.*, 2019, **152**, 762–777.

2 F. Molés, J. Navarro-Esbrí, B. Peris, A. Mota-Babiloni, Á. Barragán-Cervera and K. (Kostas) Kontomaris, Thermo-economic evaluation of low global warming potential alternatives to HFC-245fa in Organic Rankine Cycles, *Energy Procedia*, 2017, **142**, 1199–1205.

3 J. Navarro-Esbrí, F. Molés, B. Peris, A. Mota-Babiloni and K. Kontomaris, Experimental study of an Organic Rankine Cycle

with HFO-1336mzz-Z as a low global warming potential working fluid for micro-scale low temperature applications, *Energy*, 2017, **133**, 79–89.

4 F. Molés, J. Navarro-Esbrí, B. Peris, A. Mota-Babiloni, Á. Barragán-Cervera and K. (Kostas) Kontomaris, Low GWP alternatives to HFC-245fa in Organic Rankine Cycles for low temperature heat recovery: HCFO-1233zd-E and HFO-1336mzz-Z, *Appl. Therm. Eng.*, 2014, **71**, 204–212.

5 W. A. Fouad and L. F. Vega, Next generation of low global warming potential refrigerants: Thermodynamic properties molecular modeling, *AIChE J.*, 2018, **64**, 250–262.

6 C. B. Rivela, C. M. Tovar, M. A. Teruel, I. Barnes, P. Wiesen and M. B. Blanco, CFCs replacements: Reactivity and atmospheric lifetimes of a series of Hydrofluoroolefins towards OH radicals and Cl atoms, *Chem. Phys. Lett.*, 2019, **714**, 190–196.

7 P. K. Rao and S. P. Gejji, Atmospheric degradation of HCFO-1233zd(E) initiated by OH radical, Cl atom and O3 molecule: Kinetics, reaction mechanisms and implications, *J. Fluor. Chem.*, 2018, **211**, 180–193.

8 N. M. Donahue, G. T. Drozd, S. A. Epstein, A. A. Presto and J. H. Kroll, Adventures in ozoneland: Down the rabbit-hole, *Phys. Chem. Chem. Phys.*, 2011, **13**, 10848–10857.

9 D. L. Osborn and C. A. Taatjes, The physical chemistry of Criegee intermediates in the Gas Phase, *Int. Rev. Phys. Chem.*, 2015, **34**, 309–360.

10 M. I. Lester and S. J. Klippenstein, Unimolecular Decay of Criegee Intermediates to OH Radical Products: Prompt and Thermal Decay Processes, *Acc. Chem. Res.*, 2018, **51**, 978–985.

11 R. Chhantyal-Pun, M. A. H. Khan, C. A. Taatjes, C. J. Percival, A. J. Orr-Ewing and D. E. Shallcross, Criegee intermediates: production, detection and reactivity, *Int. Rev. Phys. Chem.*, 2020, **39**, 383–422.

12 F. Liu, J. M. Beames, A. S. Petit, A. B. McCoy and M. I. Lester, Infrared-driven unimolecular reaction of CH3CHOO Criegee intermediates to OH radical products, *Science (80-.).*, 2014, **345**, 1596–1598.

13 Y. Fang, F. Liu, V. P. Barber, S. J. Klippenstein, A. B. McCoy and M. I. Lester, Deep tunneling in the unimolecular decay of CH3CHOO Criegee intermediates to OH radical products, *J. Chem. Phys.*, 2016, **145**, 234308.

14 V. P. Barber, S. Pandit, V. J. Esposito, A. B. McCoy and M. I. Lester, CH Stretch Activation of CH3CHOO: Deep Tunneling to Hydroxyl Radical Products, *J. Phys. Chem. A*, 2019, **123**, 2559–2569.

15 M. J. Newland, A. R. Rickard, T. Sherwen, M. J. Evans, L. Vereecken, A. Muñoz, M. Ródenas and W. J. Bloss, The atmospheric impacts of monoterpene ozonolysis on global stabilised Criegee intermediate budgets and SO2 oxidation: Experiment, theory and modelling, *Atmos. Chem. Phys.*, 2018, **18**, 6095–6120.

16 H. Li, Y. Fang, N. M. Kidwell, J. M. Beames and M. I. Lester, UV Photodissociation Dynamics of the CH3CHOO Criegee Intermediate: Action Spectroscopy and Velocity Map Imaging of O-Atom Products, *J. Phys. Chem. A*, 2015, **119**, 8328–8337.

17 T. N. V Karsili, B. Marchetti, M. I. Lester and M. N. R. Ashfold, Electronic Absorption Spectroscopy and Photochemistry of Criegee Intermediates, *Photochem. Photobiol.*, 2022, DOI: https://doi.org/10.1111/php.13665.

18 and D. J. F. , M. J. Frisch, G. W. Trucks, H. B. Schlegel, G. E. Scuseria, M. A. Robb, J. R. Cheeseman, G. Scalmani, V. Barone, G. A. Petersson, H. Nakatsuji, X. Li, M. Caricato, A. V. Marenich, J. Bloino, B. G. Janesko, R. Gomperts, B. Mennucci, H. P. Hratchian, J. V, Gaussian 16, Revision C.01, *Gaussian Inc. Wallingford CT*.

19 H.-J. Werner, P. J. Knowles, G. Knizia, F. R. Manby and M. Schütz, Molpro: a general-purpose quantum chemistry program package, *WIREs Comput. Mol. Sci.*, 2012, **2**, 242–253.

20 H.-J. Werner, P. J. Knowles, G. Knizia, F. R. Manby, M. Schütz, P. Celani, W. Györffy, D. Kats, T. Korona, R. Lindh, A. Mitrushenkov, G. Rauhut, K. R. Shamasundar, T. B. Adler, R. D. Amos, S. Bennie, A. Bernhardsson, A. Berning, D. L. Cooper, M. J. O. Deegan, A. J. Dobbyn, F. Eckert, E. Goll, C. Hampel, A. Hesselmann, G. Hetzer, T. Hrenar, G. Jansen, C. Köppl, S. J. R. Lee, Y. Liu, A. W. Lloyd, Q. Ma, R. A. Mata, A. J. May, S. J. McNicholas, W. Meyer, T. F. M. III, M. E. Mura, A. Nicklass, D. P. O'Neill, P. Palmieri, D. Peng, K. Pflüger, R. Pitzer, M. Reiher, T. Shiozaki, H. Stoll, A. J. Stone, R. Tarroni, T.

Thorsteinsson, M. Wang and M. Welborn, MOLPRO, version 2018.1, a package of ab initio programs.

21 L. Vereecken, A. Novelli and D. Taraborrelli, Unimolecular decay strongly limits the atmospheric impact of Criegee intermediates, 2017, **19**, 31599–31612.

22 L. Vereecken, A. Novelli, A. Kiendler-Scharr and A. Wahner, Unimolecular and water reactions of oxygenated and unsaturated Criegee intermediates under atmospheric conditions, *Phys. Chem. Chem. Phys.*, 2022, **24**, 6428–6443.

23 M. Barbatti, G. Granucci, M. Persico, M. Ruckenbauer, M. Vazdar, M. Eckert-Maksić and H. Lischka, The on-the-fly surface-hopping program system Newton-X: Application to ab initio simulation of the nonadiabatic photodynamics of benchmark systems, *J. Photochem. Photobiol. A Chem.*, 2007, **190**, 228–240.

24 M. Barbatti, M. Ruckenbauer, F. Plasser, J. Pittner, G. Granucci, M. Persico and H. Lischka, Newton-X: a surface-hopping program for nonadiabatic molecular dynamics, *Wiley Interdiscip. Rev. Comput. Mol. Sci.*, 2013, **4**, 26–33.

25 V. P. Barber, S. Pandit, A. M. Green, N. Trongsiriwat, P. J. Walsh, S. J. Klippenstein and M. I. Lester, Four-Carbon Criegee Intermediate from Isoprene Ozonolysis: Methyl Vinyl Ketone Oxide Synthesis, Infrared Spectrum, and OH Production, *J. Am. Chem. Soc.*, 2018, **140**, 10866–10880.

26 G. Wang, T. Liu, A. Caracciolo, M. F. Vansco, N. Trongsiriwat, P. J. Walsh, B. Marchetti, T. N. V Karsili and M. I. Lester, Photodissociation dynamics of methyl vinyl ketone oxide: A four-carbon unsaturated Criegee intermediate from isoprene ozonolysis., *J. Chem. Phys.*, 2021, **155**, 174305.

27 J. C. McCoy, B. Marchetti, M. Thodika and T. N. V. Karsili, A Simple and Efficient Method for Simulating the Electronic Absorption Spectra of Criegee Intermediates: Benchmarking on CH2OO and CH3CHOO, *J. Phys. Chem. A*, 2021, **125**, 4089–4097.

28 V. J. Esposito, T. Liu, G. Wang, A. Caracciolo, M. F. Vansco, B. Marchetti, T. N. V. Karsili and M. I. Lester, Photodissociation Dynamics of CH2OO on Multiple Potential Energy Surfaces: Experiment and Theory, *J. Phys. Chem. A*, 2021, **125**, 6571–6579.

29 E. Antwi, R. Bush, B. Marchetti and T. Karsili, A Direct Dynamics Study of the Exotic Photochemistry of the Simplest Criegee Intermediate, CH2OO, *Phys. Chem. Chem. Phys.*, 2022, **24**, 16724–16731.

30 E. Antwi, J. M. Ratliff, M. N. R. Ashfold and T. N. V. Karsili, Comparing the Excited State Dynamics of CH2OO, the Simplest Criegee Intermediate, Following Vertical versus Adiabatic Excitation, *J. Phys. Chem. A*, 2022, **126**, 6236–6243.

31 E. Antwi, N. A. Packer, J. M. Ratliff, B. Marchetti and T. N. V. Karsili, Insights into the Ultrafast Photodissociation Dynamics of Isoprene Derived Criegee Intermediates, *Photochem. Photobiol.*, 2022, DOI: https://doi.org/10.1111/php.13736.

32 G. Wang, T. Liu, M. Zou, C. A. Sojdak, M. C. Kozlowski, T. N. V Karsili and M. I. Lester, Electronic Spectroscopy and Dissociation Dynamics of Vinyl-Substituted Criegee Intermediates: 2-Butenal Oxide and Comparison with Methyl Vinyl Ketone Oxide and Methacrolein Oxide Isomers, *J. Phys. Chem. A*, 2023, **127**, 203–215.

33 J. C. Butcher, A Modified Multistep Method for the Numerical Integration of Ordinary Differential Equations, *J. ACM*, 1965, **12**, 124–135.

34 J. W. Park and T. Shiozaki, Analytical Derivative Coupling for Multistate CASPT2 Theory, *J. Chem. Theory Comput.*, 2017, **13**, 2561–2570.

35 T. Shiozaki, BAGEL: Brilliantly Advanced General Electronic-structure Library, *Wiley Interdiscip. Rev. Comput. Mol. Sci.*, 2018, **8**, e1331.

36 Y. Fang, F. Liu, V. P. Barber, S. J. Klippenstein, A. B. McCoy and M. I. Lester, Communication: Real time observation of unimolecular decay of Criegee intermediates to OH radical products, *J. Chem. Phys.*, 2016, **144**, 61102.

37 V. J. Esposito, O. Werba, S. A. Bush, B. Marchetti and T. N. V. Karsili, Insights into the Ultrafast Dynamics of CH2OO and CH3CHOO Following Excitation to the Bright $1\pi\pi^*$ State: The Role of Singlet and Triplet States, *Photochem. Photobiol.*, 2021, **98**, 763–772.

38 E. Antwi, R. Bush, B. Marchetti and T. Karsili, A direct dynamics study of the exotic photochemistry of the simplest Criegee

intermediate, CH2OO, *Phys. Chem. Chem. Phys.*, 2022, **24**, 16724–16731.